VOL. 24, NO. 2, 2025, 167-175
elektrika.utm.my
ISSN 0128-4428

ELEKTRIKA
Journal of Electrical Engineering

Parametric Analysis of Meat-Grinder Circuits: Insights into Design and Performance Optimization

Ayaz Ahmed[1*], **Zulkurnain Abdul-Malek**[1*], **Hasmat Malik**[2*] and **Umar Ali Benisheikh**[1]

[1]Institute of High Voltage & High Current, Universiti Teknologi Malaysia, 81310 UTM Skudai, Johor, Malaysia.
[2]Faculty of Electrical Engineering, Universiti Teknologi Malaysia, 81310 UTM Skudai, Johor, Malaysia.

[*]Corresponding author: hasmat@fke.utm.my, zulkurnain@utm.my

Abstract: The meat grinder serves as a fundamental circuit for inductive pulsed-power supply (IPPS). Several derivative circuits have been constructed and suggested based on a meat grinder, including inverse commutation with semiconductor devices (ICCOS), self-charged capacitor and thyristor (SECT), capacitor pulse forming unit (CPFU), and auto-charging commutating capacitor (ACC). This research presents a simulation-based parametric investigation in which capacitance and pre-charging voltage are modified from 100 µF to 800 µF and from 600 V to 1200 V, respectively, with a full analysis of load current characteristics observed. It was noted that load current rises with an increase in capacitance or pre-charging voltages; however, with ACC-based architecture, load current diminishes as capacitor size grows. The ICCOS-based topology exhibited elevated load peaks of 9.26 kA and 16.12 kA for the first and second peaks, respectively, at 800 µF and 1200 V.

Keywords: meatgrinder, inductive pulse power supply, inverse commutation with semiconductor devices (ICCOS), self-charged capacitor and thyristor (SECT), pulse power supply

Article History: received 10 December 2024; accepted 28 February 2025; published 31 August 2025

1. INTRODUCTION

Inductive pulsed power supplies (IPPS) have higher energy densities than capacitive ones, and have greater potential which make them suitable for some applications. Three type IPPS circuits are designed XRAM based topological circuits of [1-5] Pulse transformer based circuits [6-12], and meatgrinder based topological circuits. The meatgrinder is a simple example of an inductive pulsed power supply architecture that uses the flux conservation principle to increase current. The meat grinder design involves many interconnected coils energized in series by an identical current source.

Opening switches are employed to sequentially disconnect the coils from the circuit, the remaining one coil connected to the load. The DC source P_S charges two connected inductors, L_1 and L_2, by toggling switch main S_1 as shown in Figure 1, Switch S_2 closes to connect the load, and switch S_1 opens to disconnect L_1 when the current attains the required value. The current in L_2 will rapidly increase if both inductors are fully connected because all of the energy in primary inductor L1 will be transferred to L_2. The load's connection to L_2 will result in a similarly quickly increasing pulse current [12].

Regretfully, to achieve complete coupling with real inductors is challenging. High voltage is mainly produced at both ends of main switch S1 when L1 is detached from the circuit because of its magnetic leakage flux, which tries to keep L1's current flowing. The abrupt transformation in current will also result in high voltage for the inductive load. Moreover, because of the back-induced electromotive force, S1 can tolerate greater voltages. We need to pay attention to the opening switch S1's request to make sure that the voltage and interrupting current in the meat grinder circuit reach the necessary levels. IAT researchers invented the meat grinder known as STRETCH. It looks like a meat grinder, but it also has a capacitor and parallel connection of thyristor and diodes. The objectives are to retrieve energy from the leakage flux and lower the current drop rate in the primary inductor. This will cause a drop in voltage across the primary switch[14-15]. Considerable progress has been achieved in recent years in our understanding of pulse power supply topology.

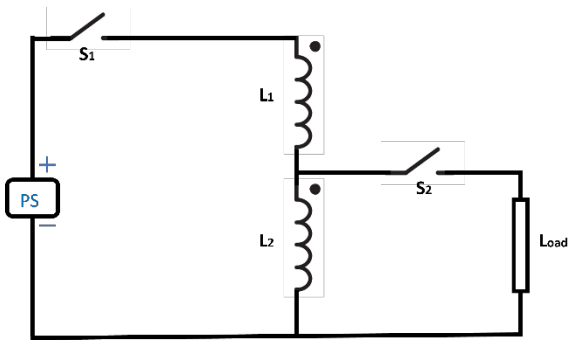

Figure 1. Meatgrinder topology [15]

The Tsinghua University designs are some of the best illustrations. The topological circuits that are known are stretch meat grinder with inverse current commutation with semiconductor (ICCOS) in which thyristors are used in this form of meat grinder to create the opening switches

[16-19], the meat grinder with self-charged capacitor thyristor (SECT) is simpler in design that uses a thyristor rather than an IGCT, in a stretch meat grinder circuit [20-21], The meat grinder with a capacitive pulsed forming unit (CPFU) [22], is known as the elementary module of capacitor-based pulsed power supplies[23-24], and the meat grinder with auto charged commutating capacitor (ACC). A meat grinder combined with ICCOS, SECT, and CPFU is the basis of pulsed generators based on capacitor-pre-charged technology [25]. Some researchers combine XRAM and meatgrinder topologies to improve the performance of the circuit [26]. All the aforementioned circuits function as expected, but the current commutating issue in none of them has been adequately fixed. Switch commutation is facilitated by the auxiliary capacitor, which provides reverse voltage and cuts off current from the primary switch [27]. To solve the pre-charging issue, Tsinghua University built a circuit that permits the auxiliary capacitor to be charged while the circuit is in operation. They use some of the energy from the primary power source which is delivered to the auxiliary capacitor earlier the inductor is charged, and at that point, pre-charging is not required.

The properties of the meat grinder-based circuits are influenced by several elements. Moreover, because the traits interact, altering one parameter frequently harms a wide range of other properties. For example, a higher inductance ratio will raise the ratio of total inductive energy to maximum capacitive energy and consequently, the current multiplication factor. Different parametric analyses are given in the literature [28], however, they are single circuit-based analyses, or they just give little inside information about the circuit parameters. To optimize the topology and create a better parametric comparison of the meat grinder-based inductive pulsed-power supply (IPPS) system, this study examined statistically the relationship between the important parameters and the meat grinder topologies' circuit performance of basic topologies including Meatgrinder with ICCOS, Meatgrinder with SECT, Meatgrinder with CPFU, and Meatgrinder with ACC[29]. Review articles in the field of IPPS were presented in literature [30-31], however, most of the reviews presented in the literature do not include the research done in past eight years and limited performance comparison is presented. In this work, a parametric analysis is presented by changing two parameters Pre-charging voltage and the charging capacitance of the meatgrinder circuits of IPPS. The analysis helps to understand the working of the circuit topologies, the effect of pre-charging voltage and charging capacitors on the performance in terms of load current characteristics of the circuit. It will further help researcher and designers to design IPPS considering the provided analysis. The flow of this work presents basics working of circuit topologies, research methodology, parametric analysis, comparative analysis, and finally conclusion as shown in Figure 2.

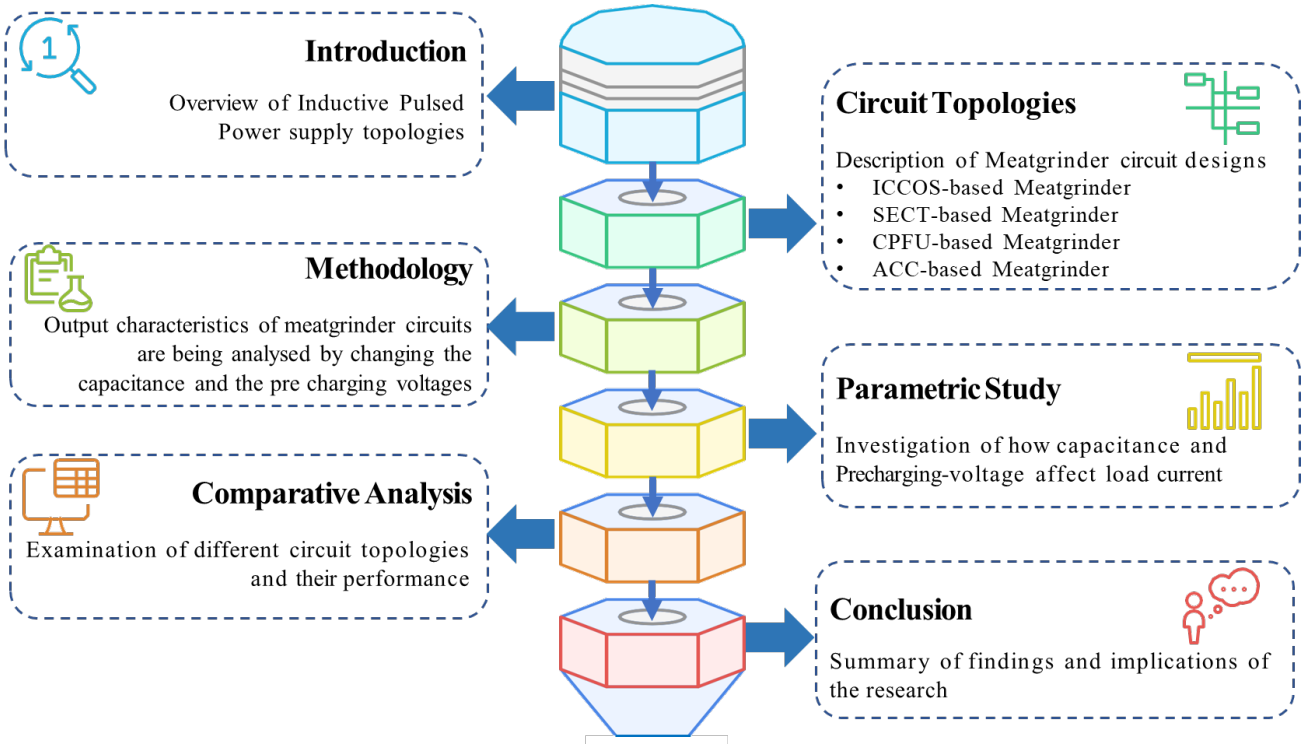

Figure 2. Representation of the Work Flow of the Study

2. BASICS OF MEATGRINDER-BASED TOPOLOGICAL CIRCUITS

2.1 ICCOS-based Stretch Meatgrinder

The STRETCH meat grinder circuit employs IGCT as the primary switch because of its vulnerability and limited current turn-off capacity. The charging current of this circuit is constrained to the maximum regulated turn-off current of the IGCT, about 4 kA. Tsinghua University improved the STRETCH meat grinder circuit's capacity by replacing the IGCT with a thyristor as the primary switch and incorporating the ICCOS subcircuit to disable the main

switch, as thyristors cannot be actively turned off. The current capacity of thyristors surpasses that of IGCTs; yet, the difficulty of deactivating them remains significant. The notion of deactivating a thyristor using the ICCOS subcircuit in the XRAM circuit was developed by ISL. The 28-kA current was suppressed using ICCOS [4]. Tsinghua University first executed the ICCOS subcircuit within a meat-grinder-based circuit. The newly assigned circuit is the STRETCH meat grinder with ICCOS, as seen in Figure 3.

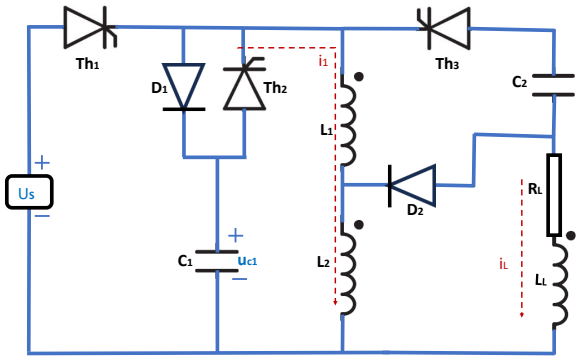

Figure 3. ICCOS-based Stretch Meatgrinder [17]

2.2 SECT based Meatgrinder

The core principle of ICCOS is applying a reverse voltage to the thyristor, so allowing it to be deactivated by a precharged capacitor. The thyristor will deactivate when the reverse voltage duration exceeds its reverse recovery time, often less than 100 µs for fast thyristors. The STRETCH meat grinder features the ICCOS circuit, a thyristor Th3, and a replenished capacitor C2 within the ICCOS circuit as shown in Figure 4. Meat grinder with SECT technology. ICCOS subcircuit. When Th1 necessitates inactivation, TH3 is activated. The current through Th1 rapidly decreases to zero, and the voltage across Th1 is negative. Th1 will deactivate if the negative voltage endures past its reverse recovery time. Upon deactivation of Th1, the circuit functions similarly to the STRETCH meat grinder [20]. The ICCOS subcircuit increases current capacity and simultaneously elevates circuit complexity.

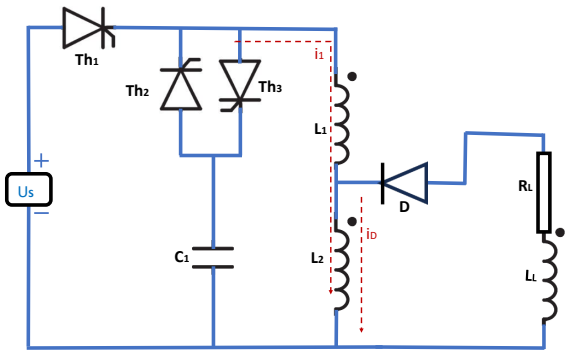

Figure 4. SECT based Meatgrinder [20]

2.3 CPFU based Meatgrinder

The CPUF branch consists of two thyristors, one inductor, and one capacitor, as seen in Figure 5. This design optimises the energy transfer mechanism and optimize operational efficiency [22]. The CPFU circuit differentiates itself from conventional circuits by immediately delivering energy to the load, hence obviating the necessity for precharged capacitors. This method mitigates problems related to elevated currents and the risk of switch damage. In the CPFU designs, the auxiliary capacitor is charged simultaneously with the circuit's operation, thereby obviating the necessity for precharging. This alteration enhances the efficiency and dependability of the meat grinder circuit.

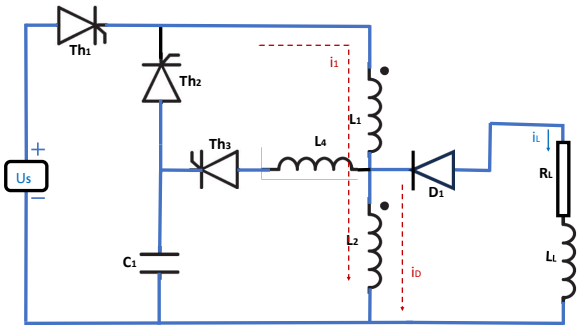

Figure 5. CPFU based Meatgrinder [22]

2.4 ACC based Meatgrinder

The newly designed circuit enables concurrent charging of the auxiliary capacitor and the inductors. Diverting a segment of energy from the primary power source to the auxiliary capacitor prior to inductor charging obviates the need for precharging, as seen in Figure 6. Considering that the precharged energy of the auxiliary capacitor is considerably less than the energy provided by the primary power source to the inductor, this energy transfer mechanism is anticipated to exert a negligible effect on energy conversion efficiency [29].

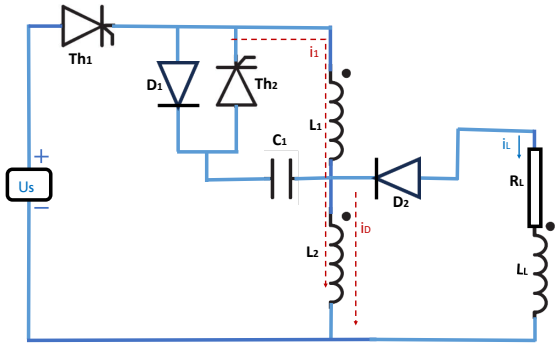

Figure 6. ACC based Meatgrinder [29]

3. METHODOLOGY PARAMETRIC STUDY OF MEATGRINDER CIRCUITS

This study examines four fundamental meatgrinder circuit topologies, focusing on the impact of varying the pre-charging voltage of the capacitor and the capacitance of the primary capacitor. The pre-charging voltage range in this study is 600 to 1200 volts, incremented by 200 volts, while the pre-charging capacitor range is from 100 microfarads to 800uF, adjusted in steps of 100uF as listed in Table 1. To observe the load current characteristics of meatgrinder

circuits the inductive parameters of all circuits were kept constant for each circuit, coupling coefficient, load inductor, load resistance, and the timing of the circuit switching circuits maintained and certain parameters were maintained constantly to observe the behavior of the circuit topologies in a comparable fashion. Table 1 presents an in-depth overview of the parameters employed in this investigation.

Table 1. Basic Parameters used in this study

Categories	Parameters	Value
Primary Source	Primary Voltage	300V
	Primary current	1000
	Pre-charged voltage	600, 800,1000, 1200V
Energy storage	Primary inductance L1	5 mH
	Secondary inductance L2	0.1 mH
	Coupling coefficient	95%
	Total inductance Ltot	7.2454mH
	Capacitance C1	100uF to 800uF
Load	Inductance LL	1uH
	Resistance RL	1.5mR
Switching Time	t0, t1, t2 (msec)	20, 25,30

Ansys Twin builder software is used to construct and simulate the meatgrinder topological circuits with some fixed parameters. Each circuit was simulated individually by selecting capacitor values and pre-charging voltages from the list. After that the result was observed and noted. Finally, a comparison between the current responses of topological circuits is investigated. A complete flow diagram of methodology used in this work is shown in Figure 7. Flow starts with the selection of circuit topology, after selecting circuit a pre-charging voltage of 600V is applied and the capacitance is selected from 100uF to 800uF with an increase of 100uF. This process is repeated for each pre-charging voltage of 800V, 1000, and 1200V and also for each topological circuit. At the end the results are compared and presented in tabular and graphical form.

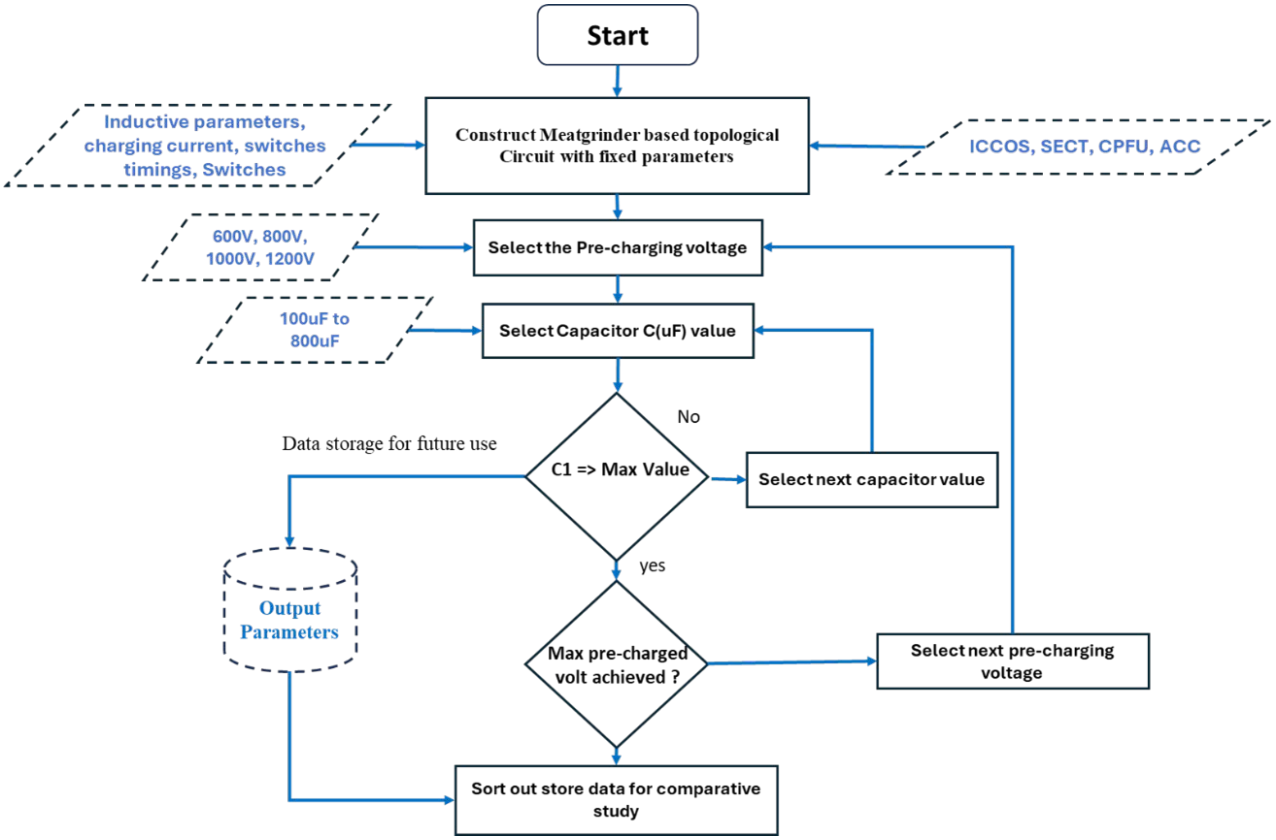

Figure 7. Illustration of proposed methodology used in this work

4. PARAMETRIC STUDY OF MEATGRINDER CIRCUITS

4.1 Response of ICCOS based Meatgrinder

The ICCOS topology shows that load current peaks (I_L) keep going up as capacitor values go from 100uF to 800uF, with a precharged voltage range of 600V to 1200V. At 600V, the first load current peak increases from 7.438 kA to 7.784 kA, while the second load current peak rises from 12.338 kA to 13.533 kA. At low precharged voltages, the load current is adequate to support the loads and rises with increasing capacity. The increase in overall efficiency is more significant at a precharged voltage of 800 V. The initial load current peak increased from 7.593 kA to 8.313 kA, while the subsequent load current peak rose from 12.644 kA to 14.454 kA. The notable rise in load currents

demonstrates a robust correlation with the system's capacity to handle substantial currents at elevated precharged voltages. This trend persists at precharged voltages of 1000V and 1200V. The initial peaks of the load current increase from 7.768kA to 8.752kA with an increase in capacitor value, while the second load current peak rises from 12.962kA to 15.247kA. As capacitance increases, the current load reaches 9.260kA for the first peak and 16.12kA for the second. When both the precharged voltage and capacitance elevate, the ICCOS topology markedly increases the load current peaks. The information in Figure 8shows a steady upward linear trend that goes along with rising capacitances and pre-charging voltages. This suggests that this topology works especially well for systems that need to boost currents by a lot.

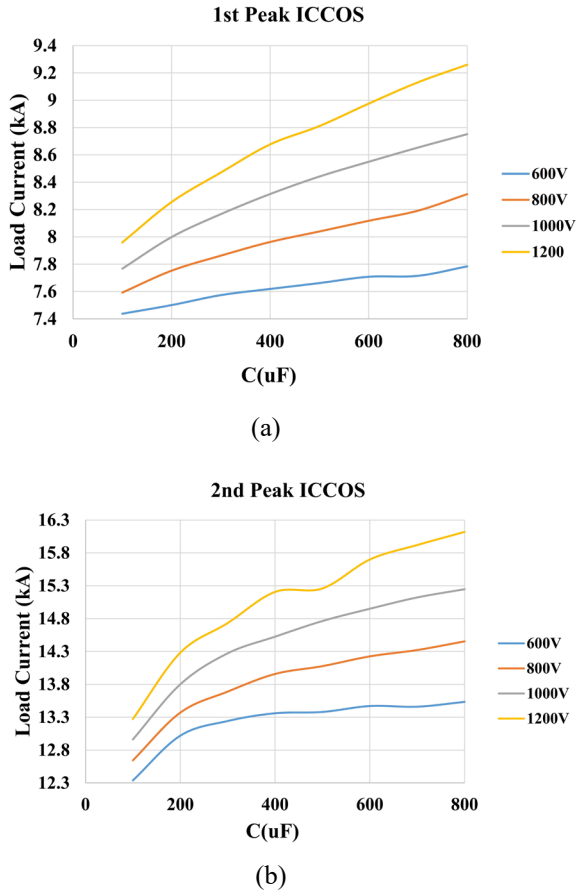

Figure 8. Response of ICCOS-based meatgrinder circuit (a) 1st Peak, (B) 2nd Peak values with capacitor change

4.2 Response of SECT based Meatgrinder

Using this data observed by the simulation study, the performance of the SCET topology at various capacitor values and pre-charged voltages (600 V, 800 V, 1000 V and 1200 V) with baseline current peaks and load current peaks at two different points. This analysis investigates how SECT topology behaves under various electrical conditions. The load current pulses in SECT based meatgrinder circuit topology also have two peaks, the first peak is smaller than second peak in each case. When the capacitor is pre-charged at a voltage of 600 V, the SCET topology delivers first load current peaks from 7.016kA to 7.186kA and second peak ranges from 12.524kA to 12.71kA. However, the increase in the first peak case is 170A and 186A for the second peak respectively. This difference in the peak currents increases as the pre-charging voltages increase from 600V to 1200V, which can be seen in Figure 9. Both peaks of load current increase from 7.078 to 7.315, and 12.773 to 12.95 when the capacitor is pre-charged to 800V.

The peak of load current is 7.161 kA and 12.683 kA at 700uF, and at 800uF, the first peak drops significantly to 1.186kA, and the second peak is 12.71 kA. A sharp drop in the initial load current peak at 800uF the behavior of the circuit is stable.

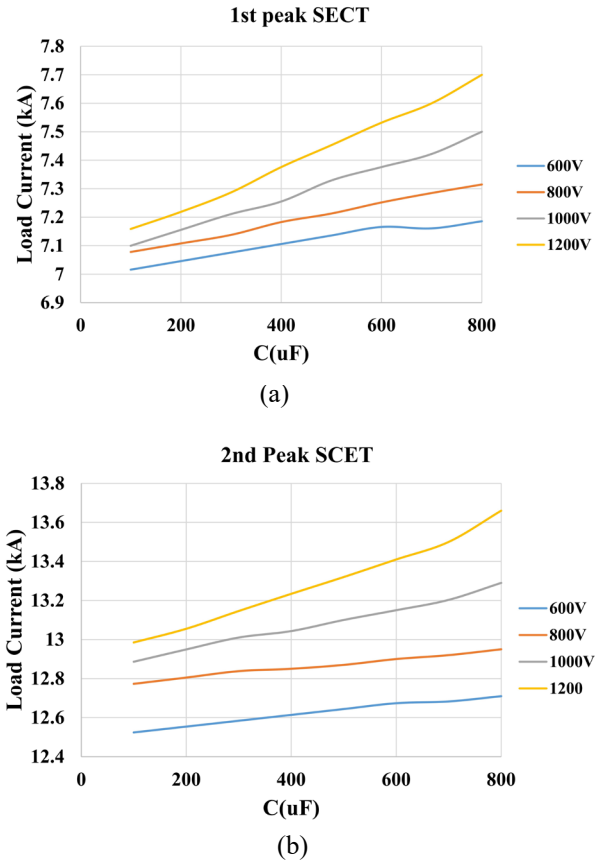

Figure 9. Response of SECT-based Meatgrinder Circuit (a) 1st Peak, (B) 2nd Peak values with capacitor change

When the pre-charge voltage rises to 800 V, the SECT topology works more stably and consistently. The current peak of the first load increased from 7.183 ka to 7.315 ka, and the second peak increased from 12.9 ka to 12.95 ka. These values indicate a more stable operation than the 600 V case, and with an increase in capacitor values, the peaks of both the primary and load current increase.

Moreover, the SECT topology performs even better and is more stable at 1200 V precharged voltage. The first load current peak rises from 7.287 ka to 7.7 ka and the second peak from 13.146 ka to 13.66 ka. The increase in current peak with high capacitor values and pre-functions voltage indicates that CECT topology can effectively control high energy levels and can be used in applications that need constant and stable high current amplification and suitable for application where the complexity of the system remains

unwanted.

4.3 Response of CPFU based Meatgrinder

It analyzes the load current peaks for CPFU topology at various capacitor values and preloaded voltages (600 V, 800 V, 1000 V and 1200 V). An in-depth analysis of the performance of the CPFU topology in different electrical situations is carried out. Performance measurements of the capacitor range from 100uF to 800uf, and pre-charged voltages remain the same for the CPFU topology. Considering pre-charged voltage 600V the circuit response at a range of capacitor values, the load currents range from 6.999kA to 7.193kA and 8.543 to 8.855kA for the first and second peaks respectively as shown in Figure 10, the response shows the linear response in all ranges. This shows stable performance with a small increase in load current peaks as the values of the capacitors increase given low preloaded voltages.

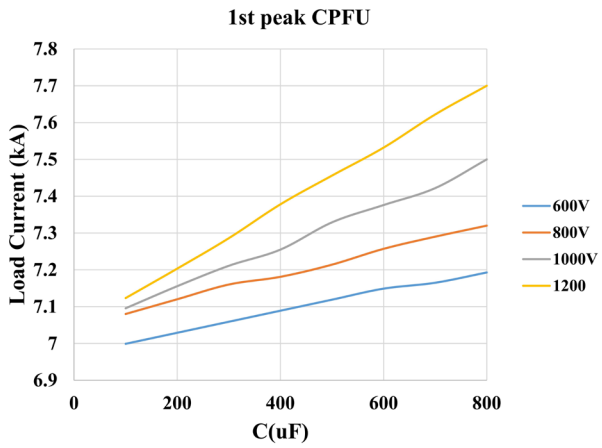

(a)

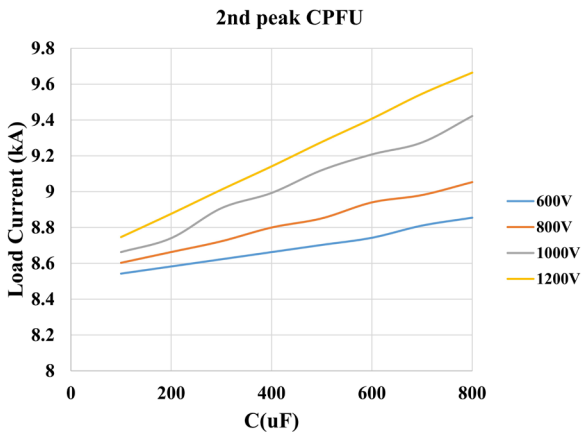

(b)

Figure 10. Response of CPFU-based Meatgrinder Circuit (a) 1st Peak, (B) 2nd Peak values with capacitor change

The CPFU topology has stable performance with a wider range of detailed data when the pre-charge voltage rises to 800 V, it slowly rises at 800uF. First load current peak increases from 7.08kA at 100uF to 7.32kA at 800uF while second peak rises to 9,053kA at that range. The first load current peaks difference that was observed 193A, 240A, 404A, and 576A at 600V, 800V, 1000V, and 1200V pre-charging voltages respectively. However, the response shows higher difference in second load current peaks. For 1000V pre-charging, the current load peak was 8.6629kA to 9.422kA, while at 1200V it was increased to 8.7466kA to 9. 664kA. The ability for increasing energy levels to be handled is demonstrated by this continuous increase of current peaks with high capacitor values and pre-charge voltage, and future applications that demand stable, sufficient current transmission will benefit from this topology.

4.4 Response of ACC-based Meatgrinder Circuit

This topological circuit used an autocharging system of capacitor so there is no need for any pre-charging voltage. So we simulate the circuit by varying the capacitors from 100uF to 800uF. The load current peak decreases as capacitor increases, from 13.165kA to 7.175kA for capacitance or 100uF to 800uF respectively. As shown in the Figure 11.

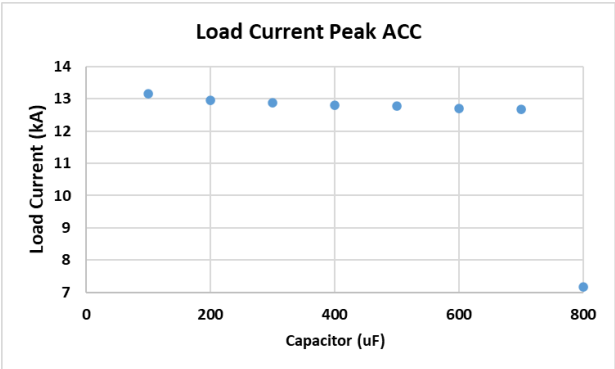

Figure 11. Response of ACC-based Meatgrinder

5. COMPARATIVE STUDY

A comparative analysis is done by considering the pre-charging voltage 1200A and capacitors ranging from 100uF to 800uF for all circuits except for the ACC meat grinder as it does not work on pre-charging voltages. The response of all basic circuits is shown in Table 2. Analysing the metrics uncovers a range of performance patterns that emerge with increasing capacitance, highlighting noteworthy differences in adaptability and overall system efficiency. These trends are particularly evident when capacitance levels rise. Both in absolute terms and in the relationship between peak load current and capacitance values, it's clear that the ICCOS and SECT based circuit's first peaks typically exhibit superior characteristics as shown in Figure 12, where the ICCOS based circuit exhibits better characteristics on all values of the capacitors and pre-charged voltages. A strong correlation between output characteristics and capacitance has been established, stemming from their enhanced flexibility and dynamic response, which are critical for improving performance under varying operating conditions. Both the first peak of ICCOS, SECT, and CPFU based circuits show steady growth, while the second peak of ICCOS and CPFU based circuits experiences a more rapid increase due to higher capacitance values.

However, the SECT-based circuit load current peaks exhibit a lower degree of variation with capacitances as it varies only 540A, and 675A first and second peak

respectively with 100uF to 800uF. All things considered, the second load peak has consistently outperformed the first load peak in terms of magnitude, and a larger contribution to system performance has been noticed throughout.

Table 2. Response of Meatgrinder circuits on 1200V pre-charging voltage

Capacitor (uF)	ICCOS (kA)		SECT (kA)		CPFU (kA)		ACC (kA)
	1st Peak	2nd Peak	1st Peak	2nd Peak	1st Peak	2nd Peak	Single Peak
100	7.96	13.274	7.1588	12.985	7.1234	8.7466	13.165
200	8.255	14.282	7.2188	13.055	7.2034	8.8766	12.957
300	8.471	14.733	7.287	13.146	7.286	9.011	12.884
400	8.677	15.204	7.376	13.234	7.378	9.141	12.802
500	8.811	15.26	7.453	13.32	7.456	9.277	12.763
600	8.975	15.7	7.532	13.41	7.532	9.407	12.709
700	9.131	15.92	7.6	13.5	7.622	9.546	12.668
800	9.26	16.12	7.7	13.66	7.7	9.664	7.175

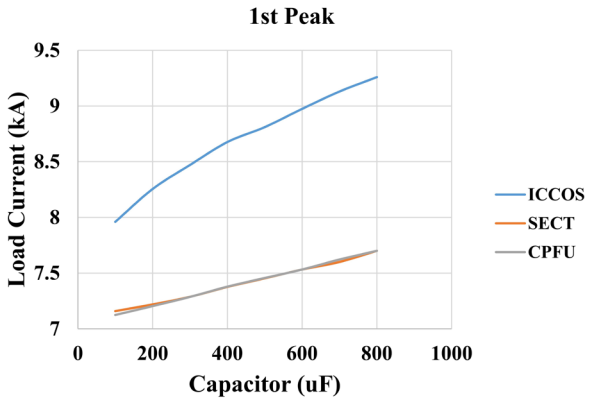

(a)

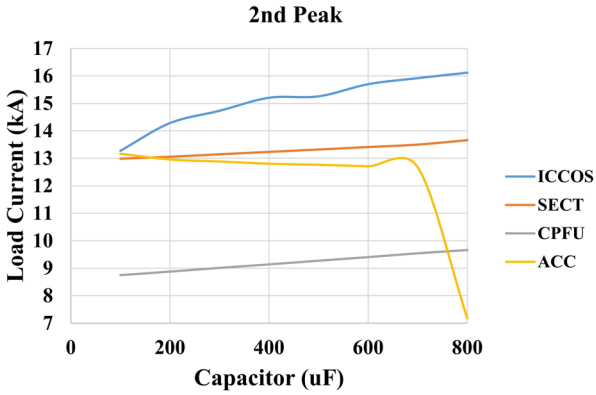

(b)

Figure 12. Load current response (a) 1st Peak, (b) 2nd Peak

However, neither of these two approaches comes near to the dynamic improvement that is observed in the second peak of ICCOS and SECT-based circuits. The ACC-based circuit load current peak, on the other hand, deviates somewhat significantly from these tendencies. Even though the peak load current values are large at lower capacitances, continue to decrease gradually with increasing capacitance, and then drop significantly to 7.175kA as the capacitor increases to 800uF, it demonstrates a significant constraint in terms of flexibility and dependability while operating at high capacitances. The pronounced disparity, on the other hand, demonstrates that second load current peaks 13.274kA to 16.12kA and 12.985kA to 13.66kA of ICCOS and SECT respectively, have greater performance since they not only maintain their efficacy at higher capacitance but even improve it. In general, ICCOS topological circuits outperform all other circuits having higher load current peaks and performances.

6. CONCLUSION

The study examines the functionality of the four fundamental topological circuits: Meatgrinder, ICCOS, SECT, CPFU, and ACC, followed by a comprehensive comparison analysis in which essential parameters are standardised for each circuit. Only two factors are altered: capacitance, ranging from 100µF to 800µF, and pre-charged voltage, varying from 600V to 1200V. The study reveals that the ICCOS-based topological circuit exhibits more load current peaks than other circuits as maximum load current peak of 16.12kA which is 15%, 40%, and 55.5% higher than SEC, CPFU, and ACC respectively, although SECT ranks second, attaining the second largest load current peaks. A linear increase in output peak currents was noted with rising capacitances of pre-voltages; however, the ACC-based meat grinder circuit exhibits an inverse relationship, whereby increasing capacitance results in a drop in peak load current. This Review work will further increase the understanding of the circuit topologies and performance parameters with capacitive and pre-charging voltage change, and it will also help the researchers or designers to design a circuit with preset parameters for their respective application. Consequently, while constructing an inductive pulsed power supply utilizing meatgrinder topology, the capacitance parameter must be judiciously determined based on real requirements.

ACKNOWLEDGMENT

The authors would like to thank the Malaysian Ministry of Higher Education for research funding with grant number FRGS/1/2023/TK07/UTM/01/4.

REFERENCES

[1] P. Dedié, V. Brommer, and S. Scharnholz, "Twenty-stage toroidal XRAM generator switched by countercurrent thyristors," in *IEEE Transactions on Plasma Science*, Jan. 2011, pp. 263–267. doi: 10.1109/TPS.2010.2055168.

[2] P. Dedié, V. Brommer, A. Badel, and P. Tixador, "Three-stage superconducting XRAM generator," *IEEE Transactions on Dielectrics and Electrical Insulation*, vol. 18, no. 4, pp. 1189–1193, 2011, doi: 10.1109/TDEI.2011.5976114.

[3] R. D. Ford, R. D. Hudson, and R. T. Klug, "Novel Hybrid XRAM Current Multiplier," 1993.

[4] S. Ma, X. Yu, and Z. Li, "XRAM Pulse Current Generator with Magnetic Flux Compression Effect," *IEEE Transactions on Plasma Science*, vol. 45, no. 7, pp. 1190–1195, Jul. 2017, doi: 10.1109/TPS.2017.2701001.

[5] O. Liebfried and V. Brommer, "A four-stage xram generator as inductive pulsed power supply for a small-caliber railgun," *IEEE Transactions on Plasma Science*, vol. 41, no. 10, pp. 2805–2809, 2013, doi: 10.1109/TPS.2013.2257873.

[6] X. Zhang, Z. Li, H. Li, C. Zhang, and S. Liu, "A High-Temperature Superconducting Pulsed-Power Supply Circuit with ICCOS," *IEEE Transactions on Plasma Science*, vol. 46, no. 11, pp. 4023–4027, Nov. 2018, doi: 10.1109/TPS.2018.2849877.

[7] H. Li, Y. Wang, Y. Zhu, R. Wu, L. Dong, and K. Dou, "Design and testing of a high-temperature superconducting pulsed-power transformer," *IEEE Transactions on Applied Superconductivity*, vol. 22, no. 2, Apr. 2012, doi: 10.1109/TASC.2012.2185794.

[8] F. Lu, N. Jin, L. Guo, and J. Fan, "Research on Energy Recovery of Superconducting Pulsed Power Supply," *IEEE Transactions on Applied Superconductivity*, vol. 31, no. 8, Nov. 2021, doi: 10.1109/TASC.2021.3091089.

[9] H. Li, Y. Zhang, C. Zhang, M. Gao, Y. An, and T. Zhang, "A repetitive inductive pulsed power supply circuit topology based on HTSPPT," *IEEE Transactions on Plasma Science*, vol. 46, no. 1, pp. 134–139, Jan. 2018, doi: 10.1109/TPS.2017.2776564.

[10] X. Liang *et al.*, "An Improved Repetitive Inductive Pulsed Power Supply Circuit with ICCOS Technique," *IEEE Transactions on Plasma Science*, vol. 48, no. 4, pp. 1082–1087, Apr. 2020, doi: 10.1109/TPS.2020.2978553.

[11] A. Ahmed, Z. Abdul-Malek, H. Malik, and T. A. Chandio, "Development of Improved Superconducting Pulsed Power Supply using Three-Winding Pulsed Power Transformer with Energy Recovery," *International Journal of Mathematical, Engineering and Management Sciences*, vol. 10, no. 1, pp. 129–147, Feb. 2025, doi: 10.33889/IJMEMS.2025.10.1.008.

[12] J. W. K. L. Oved Zucker, "The_Meat_Grinder(1984)".

[13] S. Ma, X. Yu, and Z. Li, "Determining key parameters for the STRETCH meat grinder circuit," *IEEE Transactions on Plasma Science*, vol. 43, no. 5, pp. 1485–1490, May 2015, doi: 10.1109/TPS.2015.2413055.

[14] IEEE Nuclear and Plasma Sciences Society., *Stretch Meat Grinder: A Novel Circuit Topology for Reducing opening switch voltage stress*. IEEE, 2005.

[15] I. Lindner, J. Long, D. Girogi, and T. Navapanich, "A MEATGRINDER CIRCUIT FOR ENERGIZING RESISTIVE AND VARYING INDUCTIYE LOADS (EM GUNS)," 1986.

[16] Y. Feng, L. Dai, Z. Liang, and F. Lin, "TOPOLOGICAL RESEARCH ON INDUCTIVE PULSED POWER SUPPLY," 2021.

[17] X. Yu and X. Chu, "STRETCH meat grinder with ICCOS," *IEEE Transactions on Plasma Science*, vol. 41, no. 5, pp. 1346–1351, 2013, doi: 10.1109/TPS.2013.2247065.

[18] X. Yu and X. Chu, "Comparisons of three inductive pulse power supplies," *IEEE Transactions on Plasma Science*, vol. 41, no. 5, pp. 1340–1345, 2013, doi: 10.1109/TPS.2013.2248392.

[19] B. Zhao, T. Dai, H. Li, J. Qin, C. Hu, and P. Zhang, "A Novel HTS Pulse Transformer-Based Inductive Pulsed Power Supply Circuit With Improved ICCOS Module," *IEEE Transactions on Plasma Science*, vol. 52, no. 3, pp. 843–851, Mar. 2024, doi: 10.1109/TPS.2024.3355387.

[20] X. Yu, R. Ban, X. Liu, and Z. Li, "The Meat Grinder with SECT Circuit," *IEEE Transactions on Plasma Science*, vol. 45, no. 7, pp. 1448–1452, Jul. 2017, doi: 10.1109/TPS.2017.2705663.

[21] X. Liu, X. Yu, R. Ban, and Z. Li, "Parameter Analysis of the Energy Transfer Capacitor in the Meat Grinder with SECT Circuit," *IEEE Transactions on Plasma Science*, vol. 45, no. 7, pp. 1239–1244, Jul. 2017, doi: 10.1109/TPS.2017.2704916.

[22] X. Liu and X. Yu, "The Meat Grinder with CPFU: A Novel Circuit for Inductive Pulsed Power Supplies," *IEEE Transactions on Plasma Science*, vol. 45, no. 9, pp. 2546–2551, Sep. 2017, doi: 10.1109/TPS.2017.2739420.

[23] J. Dong *et al.*, "The 100-kJ modular pulsed power units for railgun," in *IEEE Transactions on Plasma Science*, Jan. 2011, pp. 275–278. doi: 10.1109/TPS.2010.2088406.

[24] X. Liu, X. Yu, and X. Liu, "Performance Analysis and Parameter Optimization of CPPS-Based Electromagnetic Railgun System," *IEEE Transactions on Plasma Science*, vol. 44, no. 3, pp. 281–288, Mar. 2016, doi: 10.1109/TPS.2016.2519605.

[25] X. Yu, S. Ma, and Z. Li, "System Implementation and Testing of STRETCH Meat Grinder with ICCOS."

[26] A. Aougbi, Y. Achour, A. Zaoui, and H. Menana, "Improved Architecture of an Inductive Pulsed Power Supply Based on XRAM Meat-Grinder Combination," *IEEE Transactions on Plasma Science*, vol. 51, no. 5, pp. 1270–1278, May 2023, doi: 10.1109/TPS.2023.3261741.

[27] H. Sun, X. Yu, B. Li, P. Zhu, Z. Li, and H. He, "Meat Grinder with ACC Circuit: A Novel Circuit for Inductive Pulsed Power Supplies," *IEEE Transactions on Plasma Science*, vol. 48, no. 2, pp. 566–570, Feb. 2020, doi: 10.1109/TPS.2020.2966635.

[28] S. Ma, X. Yu, and Z. Li, "Parameter analysis and optimized configuration of the PFU for inductive

storage systems," *IEEE Transactions on Plasma Science*, vol. 43, no. 5, pp. 1491–1496, May 2015, doi: 10.1109/TPS.2015.2413058.

[29] H. Sun, X. Yu, B. Li, P. Zhu, Z. Li, and H. He, "Meat Grinder with ACC Circuit: A Novel Circuit for Inductive Pulsed Power Supplies," *IEEE Transactions on Plasma Science*, vol. 48, no. 2, pp. 566–570, Feb. 2020, doi: 10.1109/TPS.2020.2966635.

[30] O. Liebfried, "Review of Inductive Pulsed Power Generators for Railguns," *IEEE Transactions on Plasma Science*, vol. 45, no. 7, pp. 1108–1114, Jul. 2017, doi: 10.1109/TPS.2017.2686648.

[31] X. Yu and X. Liu, "Review of the Meat Grinder Circuits for Railguns," *IEEE Transactions on Plasma Science*, vol. 45, no. 7, pp. 1086–1094, Jul. 2017, doi: 10.1109/TPS.2017.2705164.